PHASE TRANSITION AND ELECTRICAL PROPERTIES OF MONO-, DI-, TRI- AND TETRAALKYL (OR ARYL) AMMONIUM TETRAHALOGENOCUPRATES(II) *

A. UEHARA **, A. IIMURA, K. SHIMIZU, S. MORITA, A. YOSHIFUJI
and R. TSUCHIYA

Department of Chemistry, Faculty of Science, Kanazawa University, Kanazawa 920 (Japan)

H. IMAI, Y. UEMORI, S. NAKAGAWA and E. KYUNO

*Department of Pharmaceutical Science, School of Pharmacy, Hokuriku University, Kanazawa 920 (Japan)*

(Received 18 January 1984)

ABSTRACT

The following four series of organoammonium tetrahalogenocuprates(II) were systematically prepared: $(RNH_3)_2CuX_4$, $(R_2NH_2)_2CuX_4$, $(R_3NH)_2CuX_4$ and $(R_4N)_2CuX_4$ (where R = alkyl or aryl group; X = bromide or chloride ion). Their phase transitions and electrical properties were investigated by means of DTA, DSC, electrical conductivity measurements, and IR and UV spectrophotometries.

INTRODUCTION

Some organoammonium tetrachlorocuprates(II) such as $[(CH_3)_2-CHNH_3]_2CuCl_4$ [1–4] and $[(C_2H_5)_2NH_2]_2CuCl_4$ [2,3], have been known to undergo reversible change in color at relatively low temperatures (40–50°C) in the solid state. These phenomena are attributed to the change in coordination geometry around the copper(II) ion as shown below

Low temp. (green)
square – planar

High temp. (yellow)
distorted tetrahedral

---
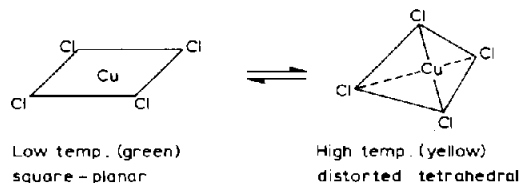
* Presented at the 47th Spring Annual Meeting of the Chemical Society of Japan, Tokyo, April 1983.
** To whom correspondence should be addressed.

TABLE 1

Analytical data for model complexes and the presence of a phase transition

Complexes [a]	Solvent [b]	C(%) Obs.	C(%) calcd.	H(%) obs.	H(%) calcd.	N(%) obs.	N(%) calcd.	Cu(%) obs.	Cu(%) calcd.	Phase transition [c]
Mono-alkyl or aryl series										
$(MeNH_3)_2CuCl_4$	Methanol	8.96	8.91	4.49	4.49	10.55	10.40	23.58	23.45	N
$(EtNH_3)_2CuCl_4$	Ethanol	16.21	16.13	5.49	5.39	9.45	9.41	21.33	21.34	N
$(EtNH_3)_2CuBr_4$	*iso*-butanol	10.10	10.11	3.30	3.39	5.92	5.89	13.52	13.37	N
$(n\text{-}PrNH_3)_2CuCl_4$	Methanol	22.17	22.13	6.23	6.19	8.52	8.60	19.59	19.52	N
$(iso\text{-}PrNH_3)_2CuCl_4$	Methanol	21.86	22.13	6.13	6.19	8.61	8.60	19.38	19.52	Y
$(PhNH_3)_2CuCl_4$	Methanol	36.15	36.61	4.04	4.10	7.06	7.11	16.13	16.14	N
$(PhCH_2NH_3)_2CuCl_4$	Methanol	39.78	39.88	4.59	4.78	6.65	6.64	14.98	15.07	N
$(PhCH_2CH_2NH_3)_2CuCl_4$	Methanol	42.72	42.73	5.40	5.38	6.50	6.23	14.02	14.13	N
Di-alkyl or aryl series										
$(Me_2NH_2)_2CuCl_4$	Methanol	16.13	16.15	5.72	5.42	9.52	9.41	21.36	20.87	Y
$(Et_2NH_2)_2CuCl_4$	Ethanol	26.96	27.14	6.83	6.79	7.96	7.92	17.83	17.96	Y
$(Et_2NH_2)_2CuBr_4$	*n*-Butanol	17.86	18.08	4.52	4.55	5.24	5.27	11.83	11.96	Y
$[PhCH_2CH_2N(Me)H_2]_2CuCl_4$	Ethanol	45.37	45.25	5.89	5.91	5.63	5.86	13.29	13.30	Y
Tri-alkyl series										
$(Me_3NH)_2CuCl_4$	Ethanol	22.19	22.13	6.14	6.19	8.52	8.60	19.52	19.74	Y
$(Et_3NH)_2CuCl_4$	Ethanol	34.88	35.16	7.68	7.81	6.81	6.84	15.30	15.51	Y
$(Et_3NH)_2CuBr_4$	Ethanol	24.53	24.53	5.53	5.49	4.86	4.77	10.79	10.82	Y
Tetra-alkyl series										
$(Me_4N)_2CuCl_4$	Methanol	27.14	27.17	6.80	6.84	7.67	7.92	17.97	18.02	N
$(Et_4N)_2CuCl_4$	Ethanol	40.83	41.25	8.47	8.65	5.98	6.01	13.35	13.64	N
$(Et_4N)_2CuBr_4$	Ethanol	29.99	29.86	6.34	6.26	4.37	4.35	9.92	9.87	N

[a] Me, Et, *n*-Pr, *iso*-Pr and Ph represent methyl, ethyl, *n*-propyl, *iso*-propyl and phenyl groups, respectively.

[b] Solvents used for the preparation and the recrystallization of the complexes.

[c] Y and N represent the presence and absence of a phase transition, respectively.

Such thermochromic behavior has so far been approached mainly from the viewpoints of spectrophotometry, magnetochemistry and structural analyses, but few studies have been devoted to examining the thermal and electrical properties associated with this behavior [5].

The Cu–Cl bonds in organoammonium tetrachlorocuprates(II) are known to be more ionic than other Cu–ligand bonds in familiar Cu(II) complexes, e.g., $[Cu(NH_3)_4(H_2O)_2]^{2+}$ [6–9]. Therefore, it is expected that the energies required to migrate the Cu^{2+} and Cl^- ions in the tetrachlorocuprates(II) may be smaller than those required to migrate the Cu^{2+} ion in the more covalent Cu(II) complexes. It may, therefore, be interesting to study electrical properties and bond characters in the organoammonium salts.

This study was therefore undertaken to (1) systematically prepare organoammonium tetrahalogenocuprates(II), (2) check the presence of a phase transition by means of DTA or DSC, and (3) investigate the change of the electrical properties accompanied by the phase transition.

The complexes in the present study are divided into four classes: monoalkyl (or -aryl) series $(RNH_3)_2CuX_4$, dialkyl (or -aryl) series $(R_2NH_2)_2CuX_4$, trialkyl series $(R_3NH)_2CuX_4$, and tetraalkyl series $(R_4N)_2CuX_4$, summarized in Table 1.

EXPERIMENTAL

Preparation of complexes

The preparative procedures for the complexes were based on those of ref. 10. The chlorides, except for $(Me_3NH)_2CuCl_4$, were prepared by mixing stoichiometric amounts of the appropriate amine hydrochloride and $CuCl_2 \cdot 2 H_2O$ in appropriate solvents (see Table 1). The resulting solution was allowed to evaporate until crystals began to appear. In the case of $(Me_3NH)_2CuCl_4$, trimethylamine hydrochloride and $CuCl_2 \cdot 2 H_2O$ were used in the ratio $3:1$, to prevent undesirable $(Me_3NH)_3CuCl_5$ and/or $(Me_3NH)_3Cu_2Cl_7$ from being deposited. The bromides were prepared by the same procedure as that for the chlorides, except that amine hydrobromides and $CuBr_2$ were used in place of amine hydrochlorides and $CuCl_2 \cdot 2 H_2O$. The analytical data for the complexes are listed in Table 1.

Spectral measurements

Visible and ultraviolet absorption spectra in the solid state were measured by a diffuse reflectance method on a Hitachi EPU-2A spectrophotometer equipped with a standard Hitachi reflection attachment. Far-IR spectra in a nujol-mull state were monitored on a JASCO IR-F far infrared spectrophotometer.
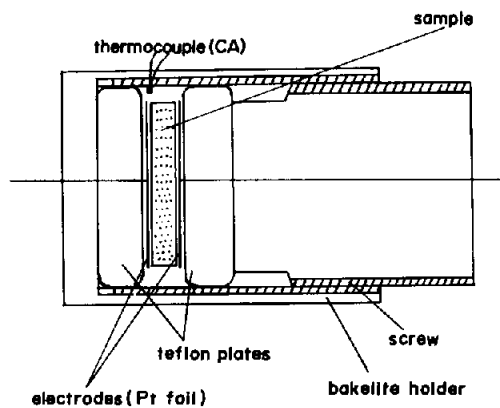
Fig. 1. Cell for measuring electrical properties.

Thermal analyses

DTA was carried out in an increasing temperature process with a MOM derivatograph (Type OD-102), and DTA and DSC curves in increasing and decreasing temperature processes were also obtained by a Rigaku Denki thermal analyser. All measurements were carried out under a constant flow of nitrogen. The enthalpy changes (ΔH) were estimated from DTA peak area as previously described [11].

Electrical measurements

For the measurements of electrical properties, samples were triturated in an agate mortar and shaped into pellets of 1 cm diameter and 0.05–0.1 cm thickness with an oil-press. The pressure used for compression was 500 kg cm^{-2}. The pellet thus formed was placed in the cell depicted in Fig. 1. The pellet was tightly sandwiched between two platinum-foil electrodes of 0.023 mm thickness. DC electrical resistivities were measured with a Takeda Riken 8651 electrometer. AC resistivities were measured with a Yokogawa universal bridge (BV-Z-13A) containing a 1 kHz oscillator. Measurements at other frequencies were conducted by the bridge provided with a wide range oscillator (model SY-107A) manufactured by NE Circuit Design Block Co. All measurements were carried out under a dry nitrogen atmosphere. The activation energies (E_a) were estimated from the slope of curves of log R_s (specific resistivity) vs. $1/T$.

RESULTS AND DISCUSSION

Examination of the presence of phase transition

DTA was applied to check the presence of a phase transition of all the complexes from their ambient temperatures to their melting points. The last
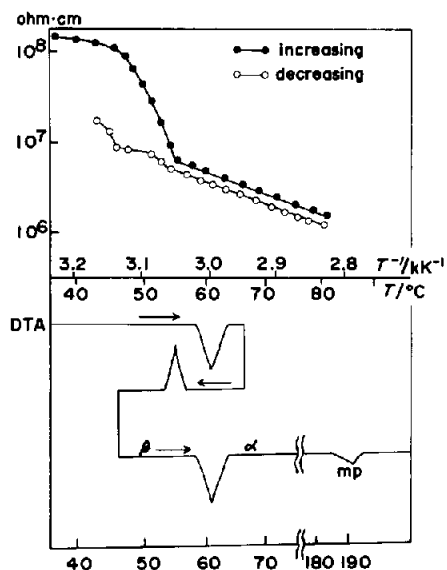
Fig. 2. Specific resistivities and DTA curve of $(Me_3NH)_2CuCl_4$ in increasing and decreasing temperature processes.

column of Table 1 shows the presence or absence of a phase transition. As seen from the table, the complexes which exhibit phase transitions are centered in the complexes of the di- and tri-substituted amine series. No phase transition was detected in the complexes of the mono- and tetra-substituted amine series except for $(iso\text{-}PrNH_3)_2CuCl_4$.

Temperature dependence of specific resistivities and DTA measurements in increasing and decreasing temperature processes

$(Me_3NH)_2CuCl_4$, $(Et_3NH)_2CuCl_4$ and $(Et_3NH)_2CuBr_4$ are representatively explained for the simplification of the following discussion.

(Me$_3$NH)$_2$CuCl$_4$

The top half of Fig. 2 shows the temperature dependence of specific resistivities of AC under 1 kHz, and the bottom half of the figure shows the DTA curve in increasing and decreasing temperature processes. With increasing temperature, the specific resistivities gradually decrease from room temperature to 45°C, and an abrupt drop of the values is observed in the range of 45–55°C where the $\beta \to \alpha$ transition * takes place; then the values again gradually decrease. The resistivities with decreasing temperature are appreciably smaller than those with increasing temperature. Such a tendency

---

* Throughout this paper, β and α represent the lower and the higher temperature modifications, respectively. The expression $\beta \to \alpha$ transition represents the transition from a β- to an α-modification.

was detected in all other complexes. This difference may be explained in two ways. First, that the transition shows hysteresis: the transition point with decreasing temperature does not appear at the same place as that with increasing temperature. Second, that the bulk character of the pellet is changed when passing the transition point: once heated above this point, grains in the pellet are held more tightly together than before heating. The pellet, after measurement, was allowed to stand overnight in a desiccator and the resistivities were rechecked. The original resistivities were recovered.

$(Et_3NH)_2CuCl_4$ and $(Et_3NH)_2CuBr_4$

Figures 3 and 4 illustrate the specific resistivities and DTA curves in increasing and decreasing temperature processes of $(Et_3NH)_2CuCl_4$ and $(Et_3NH)_2CuBr_4$, respectively. The resistivities of both the complexes decrease linearly with $1/T$ in the temperature range from room temperature to ~ 70–$80°C$ where the $\beta \rightarrow \alpha$ transition occurs. The resistivities of the chloride abruptly decrease at 75–80°C. At higher temperatures, the resistivities gradually decrease. In contrast, the resistivities of the bromide abruptly increase at about 70°C. The DTA curves of Figs. 3 and 4 show that the phase transition and the change in resistivity appear at almost the same temperature in the increasing process, whereas they appear at appreciably different temperatures from each other in the decreasing process. This tendency is parallel to that of $(Me_3NH)_2CuCl_4$.

Time dependence of DC under applied voltages

Figure 5 depicts the time dependence of DC under an applied voltage of 200 mV for α- and β-$(Me_3NH)_2CuCl_4$. As seen from the figure, the current
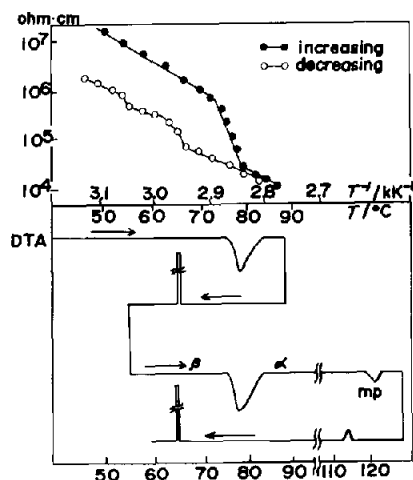

Fig. 3. Specific resistivities and DTA curve of $(Et_3NH)_2CuCl_4$ in increasing and decreasing temperature processes.
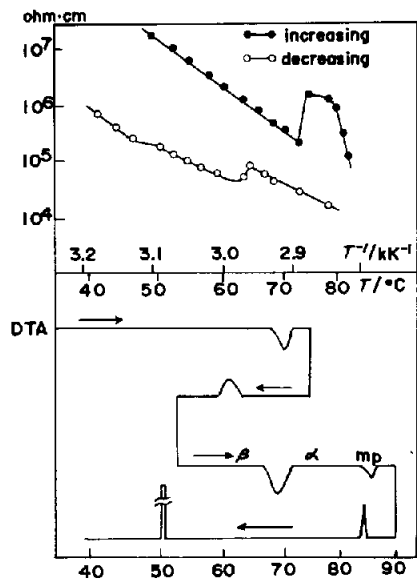
Fig. 4. Specific resistivities and DTA curve of $(Et_3NH)_2CuBr_4$ in increasing and decreasing temperature processes.

diminishes successively over several minutes. However, the current appreciably increases when the polarity of the electrodes is reversed. A similar phenomenon was found for all the complexes. This suggests that the samples are slightly polarized by the electric field and ionic conductance is partially involved in the conduction. As for β-modification, the values of DC specific resistivities were roughly equal to those of AC specific resistivities (e.g., in the case of β-$(Me_3NH)_2CuCl_4$, AC and DC resistivities are 1.70×10^7 and

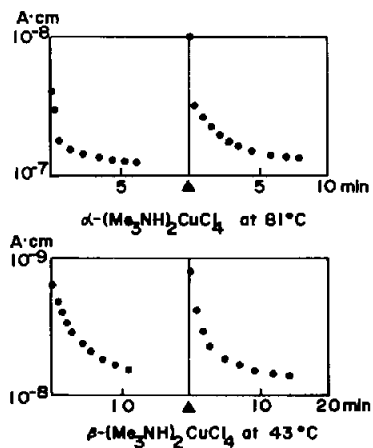Fig. 5. Time dependence of DC current under 200 mV of applied voltage for $(Me_3NH)_2CuCl_4$. (▲) At this point, the polarity of the electrodes was reversed.

2.20×10^7 ohm cm, respectively), whereas for α-modification the latter is about ten times greater than the former (e.g., in the case of α-$(Me_3NH)_2CuCl_4$ AC and DC resistivities are 1.55×10^6 and 1.26×10^7 ohm cm, respectively). This indicates that electronic conduction is predominant for β-modification, and ionic conduction is partially involved, along with electronic conduction, for α-modification.

Patterns of temperature dependence of specific resistivities

Figure 6 qualitatively illustrates the patterns of temperature dependence of AC specific resistivities of the complexes in the present study. This figure also includes the enthalpy changes for $\beta \rightarrow \alpha$ transitions ($\Delta H_{\beta \rightarrow \alpha}$) and the enthalpy changes for fusion ($\Delta H_{\alpha \rightarrow liquid}$). Four patterns can be seen in the temperature dependence of specific resistivities. (1) The specific resistivities (R_s) decrease when a $\beta \rightarrow \alpha$ transition takes place, and E_a values for an α-modification are smaller than those for a β-modification. (2) R_s values slightly increase when a $\beta \rightarrow \alpha$ transition takes place, and E_a values for an α-modification are smaller than those for a β-modification. (3) R_s values increase when a $\beta \rightarrow \alpha$ transition occurs, and E_a values for an α-modification are greater than those for a β-modification. (4) No phase transition is detectable in the temperature range from room temperature to the melting point. The mono- and tetra-substituted series fall in this type, except for $(iso\text{-}PrNH_3)_2CuCl_4$.

Let us consider the relationship between enthalpy changes and specific resistivities. In the compounds of the types (1) and (2), $\Delta H_{\alpha \rightarrow liquid}$ values are generally smaller than $\Delta H_{\beta \rightarrow \alpha}$ values. Additionally, $\Delta H_{\alpha \rightarrow liquid}$ values for complexes of types (1) and (2) are appreciably smaller than those of type (3). This implies that in complexes of types (1) and (2), the difference in entropy between the α-phase and liquid phase may not be so great, and the α-phase
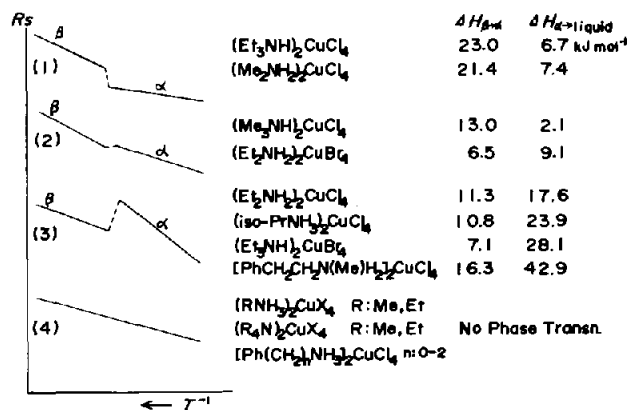

Fig. 6. Patterns of AC specific resistivities and enthalpy changes for a $\beta \rightarrow \alpha$ transition ($\Delta H_{\beta \rightarrow \alpha}$) and for fusion ($\Delta H_{\alpha \rightarrow liquid}$).

may be in a quasi-melting state *; therefore, the estimated E_a value from the log R_s vs. $1/T$ curves for the α-phase may be smaller than those for the β-phase. On the other hand, for compounds of type (3), $\Delta H_{\alpha \to \text{liquid}}$ values are larger than $\Delta H_{\beta \to \alpha}$ values, and E_a values for the α-phase are also greater than those for the β-phase. It is conceivable from these considerations that in the complexes which give relatively small $\Delta H_{\alpha \to \text{liquid}}$ values, the electrical proper-ties of the α-phase and liquid phase are fairly similar. Thus, the higher electrical conductivities and smaller E_a values are more expected for the α-phase than for the β-phase. For complexes of type (1) which give greater $\Delta H_{\beta \to \alpha}$ values, the specific resistivities are apt to decrease at the transition point, and contrary to the increase for complexes of types (2) and (3) which give relatively smaller $\Delta H_{\beta \to \alpha}$ values.

Factors influencing conductivities

Table 2 summarizes the activation energies (E_a) and the NH stretching vibration ($\tilde{\nu}_{\text{NH}}$) for the methylamine and ethylamine series. It is evident from the table that the $\tilde{\nu}_{\text{NH}}$ values tend to decrease with increasing E_a. This suggests that E_a values become smaller as the hydrogen bond between the H and Cl atoms becomes stronger (in other words the Cu–Cl bond becomes weaker). The presence of a hydrogen bond makes the repulsion of Cl–Cl smaller, and a planar geometry is preferred over tetrahedral. In general, a square planar geometry may be more favorable to contribute to electrical conduction than a tetrahedral geometry. This was also confirmed from measurements of solid-state electronic spectra. For example, in the case of (iso-PrNH$_3$)$_2$CuCl$_4$, the electronic spectrum (11600 cm^{-1}) of the green modification in the solid state (at room temperature), when heated, red-shifts to that (9100 cm^{-1}) of the yellow modification (at 77°C). The shift may be caused by the change in coordination geometry from square planar to a flattened tetrahedral species [12]. This change may be accompanied by an increase in resistivities of the complexes.

Difference in conductivities between bromides and chlorides

Table 3 lists the E_a values for the bromides and the chlorides of the ethylamine series. As seen from the table, the bromides generally have greater E_a values than the corresponding chlorides. This contradicts that predicted from the results of $\tilde{\nu}_{\text{Cu–Br}} < \tilde{\nu}_{\text{Cu–Cl}}$: the E_a values expected for the bromides may be smaller than those for the chlorides because the Cu–Br bond may be weaker than the Cu–Cl bond. This contradiction may be due to the fact that the bromide ion is not as mobile as the chloride ion because

---

* The "Quasi-melting state" is a state resembling, but not actually being, the melting state.

TABLE 2

NH stretching vibration, $\tilde{\nu}_{NH}$ (cm^{-1}), and activation energies, E_a (eV)

Methylamine series

Complexes	(MeNH$_3$)$_2$CuCl$_4$ [a]	(Me$_4$N)$_2$CuCl$_4$	(Me$_2$NH$_2$)$_2$CuCl$_4$ [a]	(Me$_3$NH)$_2$CuCl$_4$ [a]
E_a	0.86	0.96	2.73	3.12
$\tilde{\nu}_{NH}$	3150	–	3100	2770

Ethylamine series

Complexes	(EtNH$_3$)$_2$CuCl$_4$ [a]	(Et$_4$N)$_2$CuCl$_4$	(Et$_2$NH$_2$)$_2$CuCl$_4$ [a]	(Et$_3$NH)$_2$CuCl$_4$ [a]
E_a	0.44	0.44	0.91	1.23
$\tilde{\nu}_{NH}$	3170	–	3100	2800

[a] Measurements were conducted for β-modifications.

TABLE 3

Activation energies, E_a (eV), for R_2CuX_4 series

X	R = EtNH$_3$	Et$_2$NH$_2$	Et$_3$NH	Et$_4$N
Cl$^-$	0.44	0.81	1.21	0.47
Br$^-$	0.48	0.90	2.24	0.72

the bromide ion is larger and heavier than the chloride ion. Accordingly, it is conceivable that the mobility of the halide ion plays a more dominant role in electrical conduction than the strength of the Cu–X bond.

REFERENCES

1 D.N. Anderson and R.D. Willet, Inorg. Chim. Acta, 8 (1974) 167.
2 R.D. Willet, J.A. Haugen, J. Lebsack and J. Morrey, Inorg. Chem., 13 (1974) 2510.
3 R.D. Willet, O.L. Liles, Jr. and C. Michelson, Inorg. Chem., 6 (1967) 1885.
4 R.D. Willet, J.R. Ferraro and M. Choca, Inorg. Chem., 13 (1974) 2919.
5 M.A. Ahmed and M.A. Abd El-Kaffar, Thermochim. Acta, 70 (1983) 217.
6 B. Morosin and E.C. Lingafelter, J. Phys. Chem., 65 (1961) 50.
7 J.H. Russel and S.C. Wallwork, Acta Crystallogr., Sect. B, 25 (1969) 1691.
8 P.J. Lamotte-Brasseur, L. DuPont and O. Diderberg, Acta Crystallogr., Sect. B, 29 (1973) 241.
9 R.D. Willet and M.L. Larsen, Inorg. Chim. Acta, 5 (1971) 175.
10 H.E. Remy and G. Laves, Chem. Ber., 66 (1933) 401.
11 R. Tsuchiya, Y. Kaji, A. Uehara and E. Kyuno, Bull. Chem. Soc. Jpn., 42 (1969) 1881.
12 R.L. Hallow, W.J. Wells, III, G.W. Watt and S.H. Simonsen, Inorg. Chem., 13 (1974) 2106.